Revisiting Capacity Value of Variable Renewable Energy Generation in Power Systems with High Renewable Energy Penetration

Yanghao Yu, *Graduate Student Member*, *IEEE*, Haiyang Jiang, *Member*, *IEEE*, Ning Zhang, *Senior Member*, *IEEE*, Pei Yong, *Member*, *IEEE*, Fei Teng, *Senior Member*, *IEEE*, Jiawei Zhang, *Member*, *IEEE*, Yating Wang, and Goran Strbac, *Member*, *IEEE*

***Abstract*—Adequacy is a key concern of power system planning, which refers to the availability of sufficient facilities to meet demand. The capacity value (CV) of variable renewable energy (VRE) generation represents its equivalent contribution to system adequacy, in comparison to conventional generators. While VRE continues to grow and increasingly dominates the generation portfolio, its CV is becoming non-negligible, with the corresponding impact mechanisms becoming more complicated and nuanced. In this paper, the concept of CV is revisited by analyzing how VRE contributes to power system balancing at a high renewable energy penetration level. A generalized loss function is incorporated into the CV evaluation framework considering the adequacy of the power system. An analytical method for the CV evaluation of VRE is then derived using the statistical properties of both hourly load and VRE generation. Through the explicit CV expression, several critical impact factors, including the VRE generation variance, source-load correlation, and system adequacy level, are identified and discussed. Case studies demonstrate the accuracy and effectiveness of the proposed method in comparison to the traditional capacity factor-based methods and convolution-based methods. In the IEEE-RTS79 test system, the CV of a 2500 MW wind farm (with 40% renewable energy penetration level) is found to be 6.8% of its nameplate capacity. Additionally, the sensitivity of CV to various impact factors in power systems with high renewable energy penetration is analyzed.**

***Index Terms*—Power system planning, capacity value (CV), equivalent firm capacity, variable renewable energy (VRE) generation, system adequacy.**

Manuscript received: October 5, 2024; revised: January 7, 2025; accepted: March 12, 2025. Date of CrossCheck: March 12, 2025. Date of online publication: April 9, 2025.

This work was supported in part by the National Key R&D Program of China (No. 2022YFB2403300), in part by the Scientific & Technical Project of State Grid Shanghai Electric Power Company (No. SGSHDK00DWJS2310470), and in part by the Scientific & Technical Project of China Electric Power Planning & Engineering Institute (No. K202316).

Y. Yu, H. Jiang, and N. Zhang (corresponding author) are with the State Key Laboratory of Power System Operation and Control, Department of Electrical Engineering, Tsinghua University, Beijing 100084, China (e-mail: yyh20@mails.tsinghua.edu.cn; jiang_hy@tsinghua.edu.cn; ningzhang@tsinghua.edu.cn).

P. Yong is with the State Key Laboratory of Power Transmission Equipment Technology, Chongqing University, Chongqing 400044, China (e-mail: peiyong@cqu.edu.cn).

F. Teng and G. Strbac are with the Department of Electrical and Electronic Engineering, Imperial College London, SW7 2BU, London, U. K. (e-mail: f.teng@imperial.ac.uk; g.strbac@imperial.ac.uk).

J. Zhang and Y. Wang are with China Electric Power Planning & Engineering Institute, Beijing 100120, China (e-mail: jiaweizhang@eppei.com; yatingwang@eppei.com).

DOI: 10.35833/MPCE.2024.001101

I. Introduction

THE increasing penetration of variable renewable energy (VRE) and the decommissioning of conventional units are creating challenges to power system adequacy. A simple assessment of the load-carrying ability of conventional units will inevitably result in significant shortages. Therefore, evaluating the capacity contribution of VRE in future power system planning is important. However, the inherent intermittency and uncertainty of VRE resources limit their capability to provide firm power for load balancing, unlike conventional units. Effectively evaluating the adequacy contribution of VRE becomes a challenging task.

Capacity value (CV) is a measurement of the contribution of installed capacity to power system adequacy and is typically determined based on a comprehensive reliability assessment of the system [1], [2]. The ratio of CV to the nameplate capacity of the unit is its capacity credit (CC). Nevertheless, there is no precise answer for how much CV a renewable unit can provide. For example, the median marginal CV of wind resources across all regions in the US is nearly 20% when wind energy reaches a penetration level of 10%, while for photovoltaic (PV) resources, it decreases from 35% to 10% when the PV energy penetration level increases from 1% to 16% [3]. In Germany, the CV for wind resources would be 5% with a wind energy penetration level of 46% [4].

In power systems with high renewable energy penetration, there is no general consensus on the CV level that VRE units can achieve. In practical power system planning, how much VRE capacity should be considered in the load-generation balance remains an open question [5]. Accurately evaluating the CV of VRE is essential for planning power systems with high renewable energy penetration.

Assessing the CV of VRE requires solving a reliability equivalence function, which connects intermittent renewable energy generation to the firm contribution to system adequacy. Reference [6] proposed various metrics for defining CV,

among which the effective load carrying capability (ELCC) and equivalent firm capacity (EFC) are the most widely adopted for the CV of VRE [7], [8]. In practice, various reliability criteria such as loss of load probability (LOLP) and expected energy not served (EENS) are commonly used to assess system reliability. By integrating equivalence metrics with these reliability criteria, diverse definitions of CV have emerged [9].

The methods for calculating the CV of VRE can be broadly divided into analytical and simulation methods. Analytical methods employ various approximations to model reliability indices. For example, Garver's method estimated LOLP as an exponential function of the load [10], while the Z-method assumed that the surplus of available generation over peak load follows a normal distribution [11], [12]. Some methods approximated CV using the capacity factor during the hours of highest risk [3]. The IEEE PES Task Force on the CV of Wind Power recommended an iterative method based on the capacity outage probability table (COPT), which is calculated by convolving the capacities and forced outage rates of generators [2]. Reference [13] proposed a noniterative method by a discrete ELCC-LOLP table. Additionally, some studies represented the CV of VRE as a linear combination of its chronological output, weighted by the reliability of each hour [14], [15]. Reference [16] derived a closed-form expression for the ELCC of small VRE capacities. These analytical methods not only offer explicit expressions but also provide valuable insights into the factors influencing CV.

Monte Carlo (MC) simulation methods represent another mainstream approach, focusing on the probabilistic modeling of VRE generation and load curves. Reference [17] applied sequential MC simulation to calculate the ELCC of uninterruptible power supply storage. Similarly, [18] simulated the operation of PV systems through the same method and then evaluated their CVs. Generally, MC simulation methods are computationally intensive and unsuitable for direct integration into optimization models. Reference [19] comprehensively reviewed the reliability assessment methods using MC simulation variance reduction techniques.

The evaluation of the CV of VRE is essential for adequacy assessment and power balance, providing a foundation for various power system applications. It has been extensively applied in power system planning studies [9]. Incorporating a proper evaluation of the CV of VRE into planning models helps avoid overinvestment in capacity while ensuring the system adequacy. For example, [20] applied heuristic approaches to plan wind farms while considering capacity requirements. Reference [21] explored the correlation between two wind sites and introduced a combined CV model for wind site selection. Another application of CV evaluation is in capacity markets. Reference [22] used the marginal CV of VRE and storage for adequacy assessment and capacity market auctions. The combination of a well-designed market and accurate CV evaluation can effectively incentivize VRE investment to address future adequacy shortages.

In existing literature, significant progress has been made in estimating the CV of VRE. However, current studies are primarily conducted on systems with relatively low renewable energy penetration. For instance, the capacity penetration of VRE in [20] was less than 30%. Many of the simplifications used in analytical methods are prone to inaccurate estimations of the CV of VRE at higher renewable energy penetration levels [1]. MC simulation methods, however, do not provide an explicit expression for CV, making it difficult to capture the complete impact mechanisms of CV. Additionally, these methods are computationally intensive and cannot be easily integrated into optimization models. Furthermore, the impact mechanisms of the CV of VRE, especially under high renewable energy penetration levels, remain unclear. As the VRE penetration level increases, the properties of CV must be revisited. An accurate and analytical model is needed to evaluate the CV of VRE and the underlying impact mechanisms in future power systems, which can also be applied to various areas such as power system planning.

This paper revisits how increasing VRE balances the load and proposes an analytical method to evaluate the CV of VRE at a high renewable energy penetration level, which provides a cornerstone for future resource adequacy and power system planning research. The contributions of this study are as follows.

1) A general CV evaluation framework is proposed to study the CV of VRE at a high renewable energy penetration level. The properties of CV are revisited. The framework comprehensively defines and models CV based on the properties. A generalized loss function regarding the system adequacy level and the value of loss of load is proposed in this framework.

2) An analytical method for the CV evaluation of VRE is derived based on the established framework. The concise expression consists of the peak capacity factor and a correction term related to the VRE generation variance, the source-load correlation, and the system adequacy level.

3) Case studies are conducted to validate the analytical method. The saturation effect of increasing VRE capacity is demonstrated. The case studies also reveal the impact mechanisms of CV at a high renewable energy penetration level.

The remainder of this paper is organized as follows. Section II proposes the general CV evaluation framework for defining the CV of VRE and states the load-generation balance mechanisms in power systems with high renewable energy penetration to revisit the properties of CV. Based on the generalized loss function, a revisited CV model is proposed in Section III. Then, the analytical method for the CV evaluation of VRE is derived. Section IV conducts case studies, verifies the effectiveness of the proposed analytical method, and investigates the impact factors. Section V draws some conclusions.

II. Problem Statement

A. Classic CV and CC

In power system planning, CV indicates the additional adequacy that a new generation unit can provide to the power system. CC is defined as the ratio of CV to its nominal capacity [14], [23]. Generally, CV is calculated based on the equivalent reliability mechanism, which guarantees that the reliability of the system is the same as that of the system with a new VRE unit when replacing a firm generator or car-

rying an equivalent load. As the CC usually varies with capacity, it is preferable to calculate the CV directly instead of proposing a CC to represent the system adequacy contribution of the power generation unit.

Taking the EFC as an example, the reliability equivalence function of the EFC is denoted as:

$$\sum_{t=1}^{T} f_t^{\mathrm{RF}}\left(\sum_{g\in G} C_g + (w_t - P_{\mathrm{cv}}), d_t\right) = \sum_{t=1}^{T} f_t^{\mathrm{RF}}\left(\sum_{g\in G} C_g, d_t\right) \quad (1)$$

where $f_t^{\mathrm{RF}}(p,d)$ is the reliability function of the system with a total generation capability of p and load level d at time t; w_t is the time-series output of the evaluated additional unit; G is the set of existing thermal units in the system; T is the number of time periods, which is usually set to be 8760 for a full year with hourly time resolution; d_t is the time-series load of the system; C_g is the capacity of unit g; and P_{cv} is the CV of the evaluated additional unit, which is also referred to as the EFC. The reliability of the system without the evaluated unit is shown on the right-hand side of (1).

B. Load-generation Balance Mechanisms in Power Systems with High Renewable Energy Penetration

The essence of CV is to use a single value to summarize the contribution of the VRE to the power balance throughout all operation time periods. Therefore, to explore the impact mechanisms of this value, it is necessary to investigate the chronological load-generation balance, which becomes more complicated and diverse as the VRE penetration level increases. At a low VRE penetration level, the capacity requirement is mainly fulfilled by conventional units. The load loss of the system primarily comes from the forced outage of conventional units, which is represented by the time-independent COPT. The VRE generation can be fully utilized by reducing the output from the conventional units. It is appropriate to use the average VRE generation as the CV. As the VRE penetration level becomes high, the above load-generation balance mechanisms gradually change. VRE generally plays a more important role in the power balance, which indicates that VRE generation fluctuations affect the adequacy more than the forced conventional unit outages.

At a high renewable energy penetration level, the contribution of VRE to the power balance varies significantly over time. Figure 1 shows the operation curves of the VRE and thermal units from a modified IEEE-RTS79 test system during a peak load week [24].

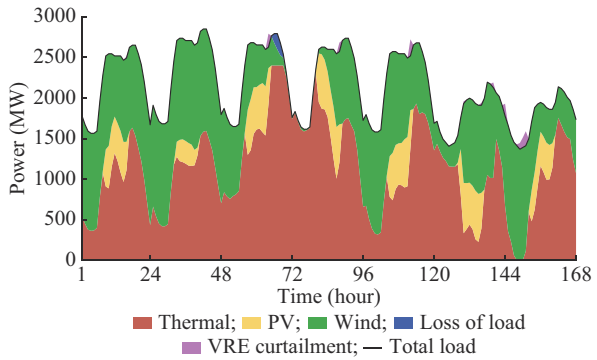

Fig. 1. Operation curves of VRE and thermal units from a modified IEEE-RTS79 test system.

In this system, the peak load is 2850 MW. The total capacity of the conventional power plants is 2400 MW, while the total capacity of VRE units is 2800 MW, with a wind-to-PV capacity ratio of 3:2. The overall VRE penetration level of the system is 50%.

During one of the peak load periods, e.g., 18:00-19:00 on Wednesday, shown as the 66$^{\mathrm{th}}$-67$^{\mathrm{th}}$ hour in Fig. 1, the total conventional unit capacity is deficient, so a large amount of VRE generation is needed. During this period, the VRE generation contributes greatly to the overall reliability in the adequacy evaluation.

Unfortunately, during this period, the VRE generation is low, so loss of load occurs. At the same time, on Tuesday, the overall generation is abundant. The peak risk is no longer entirely aligned with the peak load. The time correspondence between renewable energy and the load drives the adequacy contribution of VRE.

Moreover, even sustained high VRE generation contributes little to the CV during some low-demand periods, as the adequacy provided by conventional units is already sufficient. Therefore, during these periods, VRE primarily displaces thermal generation for the purpose of supplying green energy, rather than to enhance system adequacy. For example, in the early morning of Sunday, shown as the 149$^{\mathrm{th}}$-150$^{\mathrm{th}}$ hour in Fig. 1, the system even has to curtail some VRE generation and no thermal units are committed.

C. Properties of CV in Systems with High Renewable Energy Penetration

According to the abovementioned balance mechanisms, in power systems with high renewable energy penetration, the CV of VRE shows several novel properties, as follows.

1) The CV of VRE has a strong saturation effect as its penetration level increases. At a high renewable energy penetration level, the peak load periods do not completely indicate the peak risk periods. During some critical periods when VRE resources are limited, even a high VRE capacity is unable to fully meet the load, which results in a decreasing marginal CV (the incremental CV of the incremental VRE capacity). Figure 2 displays the scattered CV results under various thermal unit configurations in the IEEE-RTS79 test system with a peak load of 2850 MW. Each point corresponds to a random thermal unit configuration in which some thermal units are randomly added in or removed from the generation mix in the system. With increasing VRE penetration levels, the saturation effect can be observed in Fig. 2.

2) The CV of VRE highly depends on the existing system adequacy level. When the system adequacy level is high, the CV of VRE is small due to its limited contribution to an already well-balanced system. Conversely, in low-adequacy systems, VRE provides essential energy to meet the demand, resulting in a higher CV. This mechanism causes the CV to differ greatly in different studies that do not share the same system adequacy levels. Figure 2 also illustrates the variation of CV at different system adequacy levels with increasing penetration levels. For example, at 1200 MW of wind capacity, the relative deviation of CVs under different adequacy levels exceeds 30%.

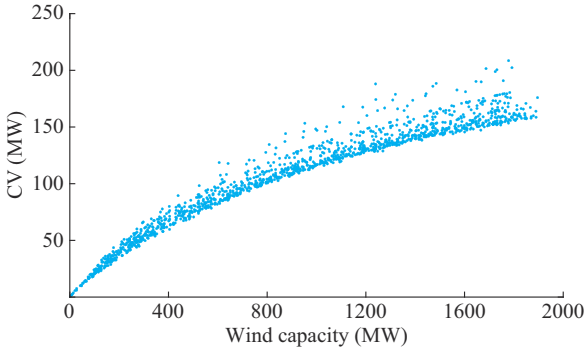

Fig. 2. CV results under various thermal unit configurations in IEEE-RTS79 test system.

3) As the VRE capacity increases, the cases in which system generation is abundant and in which the system generation is not enough can both occur because of the variation in VRE. Therefore, its capacity factor is gradually becoming less representative of its CV. The performance of a VRE unit during certain critical periods greatly influences its CV.

4) The mechanisms of the load-generation balance at a high renewable energy penetration level change. In the traditional reliability scheme, the loss of load is dominated by the time-independent forced outages of conventional units. The LOLP is always higher during the peak load periods. For systems with high renewable energy penetration, the balance mechanisms indicate that the reliability scheme is dominated by the chronological fluctuations in VRE generation rather than the availability of conventional units. Figure 2 also indicates the variation in CVs with changing thermal unit configurations under the COPT scheme. Therefore, the loss function for the load-generation balance should not rely solely on the COPT.

Considering the new properties of CV at high renewable energy penetration levels, the new CV evaluation framework should focus on the following three critical points.

1) Considering that the traditional reliability frameworks are insufficient to capture the CV fluctuation and saturation introduced by high renewable energy penetration levels, the reliability function of the loss of load should be revisited.

2) According to the second property, a system adequacy level should be predefined before evaluating the CV.

3) According to the third and fourth properties, the evaluation should focus on the critical periods of load-generation balance.

III. Revisited CV Model and Analytical Method for CV Evaluation

A. Generalized Loss Function

The reliability function $f_t^{\mathrm{RF}}(p,d)$ is essential for evaluating the CV of VRE. Typical metrics such as LOLP and EENS are widely used to assess the system reliability. These metrics are usually calculated from the COPT, which stresses the dominant role of conventional units in the system. However, the thermal unit configuration has a great impact on the COPT and, hence, the reliability metrics. More general loss functions can be defined to represent the system adequacy for calculating the CV of VRE. Based on the above understanding of the load-generation balance mechanisms, the generalized loss functions should have the following properties.

1) The generalized loss function should be a monotonic function of the total generation based on a fixed load. Considering that the outputs of conventional units are constant and time-invariant, higher VRE generation results in a smaller loss function.

2) Due to the time variation in the load demand, each time period has a unique loss function that is affected by the load level.

3) The loss function increases more rapidly as power shortages become more severe, reflecting the increasing sensitivity of the system to additional shortages. In other words, the marginal impact of each incremental shortfall of the system grows, highlighting the escalating consequences of inadequate supply. Mathematically, this implies that the second derivative of the generalized loss function should be greater than zero.

4) The generalized loss function should reflect the system adequacy level. For power systems with high renewable energy penetration, the reliability scheme is dominated by the chronological fluctuations in VRE generation. Therefore, we can focus on the loss of net load brought by the mismatch of the VRE generation and load while simplifying the output of conventional units to the fixed system adequacy level. To determine the system adequacy level, the following assumption is proposed.

Assumption 1 We use a fixed parameter G to represent the system adequacy level, which can also be interpreted as the total EFC of existing units. Loads below G can be met by the existing units with a sufficiently high probability, allowing the corresponding loss to be neglected and set to be zero.

The value of G can be obtained from the EENS value of the system $EENS_{\mathrm{system}}$ by solving the following function.

$$\sum_{t=1}^{T}(d_t-G)I(d_t-G\geq 0)=EENS_{\mathrm{system}} \tag{2}$$

where $I(S)$ is the indicator function, which returns a value of 1 if the statement S is true and 0 otherwise.

Consequently, the generalized loss function $f_t(\cdot)$ has the following standard form.

$$f_t(w_t)=g_t(w_t)I(d_t-G-w_t\geq 0)\quad \forall t \tag{3}$$

where $g_t(w_t)$ is a monotonic function that is also affected by the value of d_t. Figure 3 displays the curve of this loss function. For loads below the system adequacy level, the loss is zero, which allows the CV model to capture the VRE performance during peak load periods.

B. Model Description

The CV model can be further derived and solved using the generalized loss function. Substituting the function (3) into the definition of EFC as proposed in (1), the following equation is proposed to solve the CV of a generation unit.

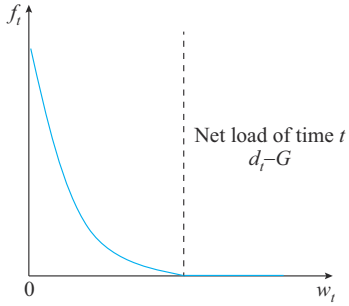

Fig. 3. Curve of generalized loss function.

$$\sum_{t=1}^{T} g_t(w_t - P_{\text{cv}}) I(d_t - G - (w_t - P_{\text{cv}}) \geq 0) = \sum_{t=1}^{T} g_t(0) I(d_t - G \geq 0) \tag{4}$$

For simplicity, we note the time-series net load as $d_t^{\text{net}} = d_t - G$. $\Omega = \{t | d_t^{\text{net}} \geq 0\}$ is applied to indicate the set of peak load periods. The set of nonpeak load periods when $d_t^{\text{net}} \leq 0$ is denoted as Ω'. Therefore, for $t \in \Omega$, $f_t(0) = g_t(0) \geq 0$; for $t \in \Omega'$, $f_t(0) = 0$. A positive d_t^{net} means that the system adequacy level cannot fully cover the load and that there is a significant probability of a load shortage with the existing units. In Ω', the loads are less than G and can be fulfilled by the existing units. The system adequacy levels inherently influence the ranges of peak load periods. In scenarios with lower system adequacy levels, the evaluation of the CV of VRE emphasizes a broader time range of VRE generation. The evaluated VRE unit is supposed to meet the general base load in providing the resource adequacy to the system. On the contrary, in scenarios with high system adequacy levels, the range of the critical peak load periods becomes smaller. The performance of VRE units in meeting these peak loads is more important in determining the CV result.

After removing the indicator function on the right-hand side, (4) is simplified as:

$$\sum_{t=1}^{T} f_t(w_t - P_{\text{cv}}) = \sum_{t \in \Omega} g_t(0) \tag{5}$$

Equation (5) is an implicit function of P_{cv}. This problem can be solved with classic iterative searching methods. In this paper, the CV results from the bisection method will serve as the benchmark result.

It should be noted that the calculation of the loss function actually spans across the whole evaluation period. It is capable of embedding intertemporal power system operations, which means that the integration of flexible resources such as energy storage and demand response is feasible in this model. As presented in [25], a model that focuses on the operational characteristics of the flexible resources can be solved as a prior process. Then, with the optimized dispatch, the net load profile can be modified and further utilized in the proposed model to quantify the CV of both VRE and flexible resources.

C. Analytical Method for CV Evaluation

Equation (5) provides a way to numerically calculate P_{cv}. This subsection further derives an analytical formula for P_{cv} to analyze its impact factors.

First, the nonlinear and nondifferentiable indicator $I(x)$ in the generalized loss function inhibits obtaining the CV solution. To address this issue, the ancillary variables u_t are defined to replace the original VRE generation w_t:

$$u_t = \begin{cases} w_t & w_t < d_t^{\text{net}} + P_{\text{cv}} \\ d_t^{\text{net}} + P_{\text{cv}} & w_t \geq d_t^{\text{net}} + P_{\text{cv}} \end{cases} \tag{6}$$

By substituting u_t into the generalized loss function, (7) holds, which results in (8).

$$g_t(u_t - P_{\text{cv}}) = \begin{cases} f_t(w_t - P_{\text{cv}}) & w_t < d_t^{\text{net}} + P_{\text{cv}} \\ g_t(d_t^{\text{net}}) = 0 & w_t \geq d_t^{\text{net}} + P_{\text{cv}} \end{cases} \tag{7}$$

$$g_t(u_t - P_{\text{cv}}) = f_t(w_t - P_{\text{cv}}) \tag{8}$$

Consequently, (5) is rewritten as:

$$\sum_{t \in \Omega} g_t(0) = \sum_{t=1}^{T} g_t(u_t - P_{\text{cv}}) = \sum_{t \in \Omega} g_t(u_t - P_{\text{cv}}) + \Delta \tag{9}$$

where Δ is the sum of the values of the generalized loss function during all nonpeak load periods.

$$\Delta = \sum_{t \in \Omega'} g_t(u_t - P_{\text{cv}}) \tag{10}$$

Second, the Taylor expansion can be performed on $g_t(u_t - P_{\text{cv}})$ at point 0:

$$g_t(u_t - P_{\text{cv}}) = g_t(0) + (u_t - P_{\text{cv}}) g_t'(0) + \frac{1}{2}(u_t - P_{\text{cv}})^2 g_t''(0) + o((u_t - P_{\text{cv}})^2) \tag{11}$$

where $g_t'(0)$ and $g_t''(0)$ are the first-order and second-order derivatives of $g_t(x)$ at point 0; and $o(\cdot)$ is the higher-order infinitesimal term.

By substituting (11) into (9) and neglecting the term of the higher-order infinitesimal, we can obtain:

$$\sum_{t \in \Omega} \left[(u_t - P_{\text{cv}}) g_t'(0) + \frac{1}{2}(u_t - P_{\text{cv}})^2 g_t''(0) \right] + \Delta = 0 \tag{12}$$

The values of $g_t'(0)$ and $g_t''(0)$ are independent of P_{cv}. Thus, for a given generalized loss function, the function with respect to P_{cv} can be obtained by calculating the derivatives of the loss function at each time t.

Third, taking the quadratic function as an example, $g_t(w_t)$ can be defined as in (13). It perfectly satisfies the aforementioned properties, and the values of its third and higher derivatives are naturally zero. The quadratic function can also quantify the value of loss of load and incorporate economic considerations into reliability needs, as mentioned in [26].

$$g_t(w_t) := \lambda (d_t^{\text{net}} - w_t)^2 \quad \forall t \tag{13}$$

where λ is a function coefficient.

Given this generalized loss function, its derivatives can be calculated and (12) becomes:

$$\lambda \sum_{t \in \Omega} [(u_t - P_{\text{cv}})(-2 d_t^{\text{net}}) + (u_t - P_{\text{cv}})^2] + \Delta = 0 \tag{14}$$

Expanding the equation and combining like terms leads to:

$$-\frac{\Delta}{\lambda} = \sum_{t \in \Omega} [2(u_t - P_{\text{cv}})(-d_t^{\text{net}}) + (u_t - P_{\text{cv}})^2] = \sum_{t \in \Omega} [P_{\text{cv}}^2 + 2(d_t^{\text{net}} - u_t) P_{\text{cv}} + u_t^2 - 2 d_t^{\text{net}} u_t] = T_\Omega P_{\text{cv}}^2 + \sum_{t \in \Omega} 2 (d_t^{\text{net}} - u_t) P_{\text{cv}} + \sum_{t \in \Omega} (u_t^2 - 2 d_t^{\text{net}} u_t) \tag{15}$$

where T_Ω is the number of time periods in set Ω.

Fourth, the statistical characteristics, such as the mean value, of the time-series values in (15) can be calculated. The net load d^{net} is treated as a single stochastic variable D^N. During each time period (typically an hour), the net load d_t^{net} is considered a sample drawn from the distribution of the stochastic variable. Similarly, the ancillary variable u_t for VRE generation is treated as the stochastic variable U. Then, $E_\Omega(D^N)$ and $E_\Omega(U)$ denote the expected value of the net load d^{net} and the ancillary variable in the time set Ω, respectively. $\sigma_\Omega^2(U)$ is the variance of the ancillary variable. Moreover, suppose that $Cov_\Omega(D^N, U)$ denote the covariance of the two stochastic variables D^N and U. All the statistical values are computed with respect to the timespan in the time set Ω. The following relations hold:

$$\begin{cases} E_\Omega(D^N) = \dfrac{\sum_{t\in\Omega} d_t^{\text{net}}}{T_\Omega} \\ E_\Omega(U) = \dfrac{\sum_{t\in\Omega} u_t}{T_\Omega} \end{cases} \tag{16}$$

$$\sigma_\Omega^2(U) = E_\Omega(U^2) - E_\Omega^2(U) \tag{17}$$

$$Cov_\Omega(D^N, U) = Cov_\Omega(D, U) = E_\Omega(D^N U) - E_\Omega(D^N)E_\Omega(U) \tag{18}$$

Combining (15)-(18), the CV function is rewritten as:

$$T_\Omega(P_{\text{cv}}^2 + 2E_\Omega(D^N - U)P_{\text{cv}} + E_\Omega^2(D^N - U) - E_\Omega^2(D^N) + \sigma_\Omega^2(U) - 2Cov_\Omega(D^N, U)) + \frac{\Delta}{\lambda} = 0 \tag{19}$$

Therefore, with known chronological load and wind power generation data, (19) establishes a quadratic equation for P_{cv}. Let $A = \sigma_\Omega^2(U) - 2Cov_\Omega(D^N, U) + \Delta/(\lambda T_\Omega)$, the analytical solution can be obtained using the root formula.

$$P_{\text{cv}} = -E_\Omega(D^N - U) + \sqrt{E_\Omega^2(D^N) - A} \tag{20}$$

Notably, the negative root is omitted in this context. Equation (20) gives the explicit and exact analytical solution of P_{cv}. The value is determined by both the statistical characteristics of the chronological VRE generation and the expected value of the peak load.

The expression for P_{cv} can be further derived with approximations as follows:

$$\begin{aligned} P_{\text{cv}} &= E_\Omega(U) + \sqrt{E_\Omega^2(D^N) - A} - E_\Omega(D^N) = \\ &E_\Omega(U) - \frac{A}{E_\Omega(D^N) + \sqrt{E_\Omega^2(D^N) - A}} \approx E_\Omega(U) - \\ &\frac{A}{2E_\Omega(D^N)} \approx E_\Omega(U) - \frac{\sigma_\Omega^2(U) - 2Cov_\Omega(D^N, U)}{2E_\Omega(D^N)} \end{aligned} \tag{21}$$

Equation (21) provides a concise analytical expression for the CV of VRE. P_{cv} is composed of two parts: the first part is the mean VRE generation during peak load periods (or the peak capacity factor, as stated in [3]), and the second part is a negative correction term related to the variation in VRE generation and the load-VRE correlation during peak load periods.

Several impact factors of the CV of VRE can be inferred from (21).

1) Installed capacity. For a small VRE installation, its CV is essentially the peak capacity factor. As the capacity increases, the correction term grows faster and leads to the saturation of the CV.

2) Output fluctuation. As the VRE generation variance increases, the value of the correction term increases, which results in a lower CV. The erratic fluctuation of the output usually results in a limited contribution of the VRE unit to the system adequacy.

3) Source-load correlation. In the correction term of P_{cv} expressed in (21), i.e., $-A/(E_\Omega(D^N) + \sqrt{E_\Omega^2(D^N) - A})$, a higher covariance of the load and VRE generation leads to a lower correction term and a higher CV. This finding fits the intuition that a stronger source-load correlation denotes better system adequacy during peak load periods.

D. Errors in Approximations

Compared with the exact solution, the explicit expression for P_{cv} in (21) introduces errors from the two approximation steps. The errors can be further quantified as follows. For simplicity, a new term, $A' = \sigma_\Omega^2(U) - 2Cov_\Omega(D^N, U)$, is defined.

$$\begin{aligned} Err &= \frac{-A'}{2E_\Omega(D^N)} - (\sqrt{E_\Omega^2(D^N) - A} - E_\Omega(D^N)) = \\ &\frac{2E_\Omega^2(D^N) - 2E_\Omega(D^N)\sqrt{E_\Omega^2(D^N) - A} - A'}{2E_\Omega(D^N)} = \\ &\frac{(E_\Omega(D^N) - \sqrt{E_\Omega^2(D^N) - A})^2 + A - A'}{2E_\Omega(D^N)} = \\ &\frac{(E_\Omega(D^N) - \sqrt{E_\Omega^2(D^N) - A})^2 + \dfrac{\Delta}{\lambda T_\Omega}}{2E_\Omega(D^N)} \end{aligned} \tag{22}$$

where Err is the overall approximation error, which can be divided by two terms $(E_\Omega(D^N) - \sqrt{E_\Omega^2(D^N) - A})^2/(2E_\Omega(D^N))$ and $\Delta/(\lambda T_\Omega \cdot 2E_\Omega(D^N))$, and the two terms are both non-negative.

The first term is introduced by the fraction approximation in (21). A larger A will result in a greater error for a given load. Both a higher VRE capacity and a greater output variety will lead to a larger A, which further increases the fraction approximation error.

The second term is determined by the generalized losses during non-peak load periods Ω'. According to the definition of EFC, the loss function at time t will be nonzero only if $d_t^{\text{net}} + P_{\text{cv}}$ is larger than w_t. At a low renewable energy penetration level, P_{cv} is usually marginal, and the vast majority of $d_t^{\text{net}} + P_{\text{cv}}$ values are negative for time t in Ω'. Therefore, this non-peak loss-related error is negligible. Moreover, a high renewable energy penetration level will lead to a high CV. Therefore, it is possible that there are some periods in Ω' when the value of the new net load $d_t^{\text{net}} + P_{\text{cv}}$ exceeds the VRE generation, which means that power shortages are likely to occur in the original non-peak load periods and that the value of Δ will increase. Consequently, a greater VRE capacity will increase the non-peak loss-related error.

IV. Case Studies

Case studies are conducted to test the performance and effectiveness of the proposed framework. First, the iterative and analytical methods for CV evaluation with the proposed loss function are applied to the IEEE-RTS79 test system. The CVs of wind and PV farms are illustrated across a range of renewable energy penetration levels from low to high. Next, according to the generation characteristics of VRE that influence its CV as revealed by the explicit CV expression, some factors impacting the CV of VRE are studied. Then, the evaluation error of the analytical method is elaborated based on the explicit error formula. Finally, the impact of the system adequacy level on the CV is discussed.

A. Case Study Data

The IEEE-RTS79 test system is used in the case study to illustrate the proposed methods [24]. The total capacity of the conventional power plants and the peak load are 3405 MW and 2850 MW, respectively. The generation-level reliability of the IEEE-RTS79 test system denoted by EENS is 1176 MWh/year. As indicated in (2), the corresponding G is calculated as 2696.6 MW. Therefore, the value of G is set to be 2700 MW in the case study. The set of peak load periods $\Omega=\{t|d_t^{\text{net}}\geq 0\}$ contains 23 time slots where the loads vary from 2707.5 MW to 2850 MW. The test is conducted with an hourly time resolution over a one-year period. The hourly wind and PV power generation output data are simulated from practical power plants located in the northwestern area of China. The average annual utilization hours of wind and PV resources are 2600 and 1700 hours, which correspond to capacity factors of 30.0% and 19.4%, respectively. Typical curves of the renewable energy data and the load data over a typical week are illustrated in Fig. 4.

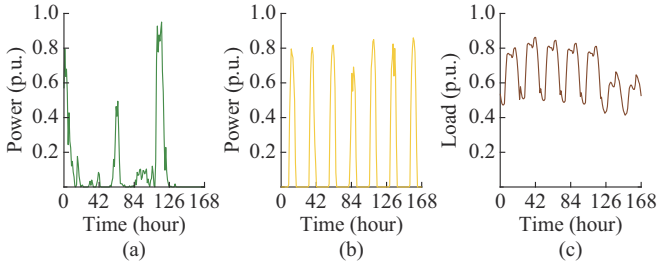

Fig. 4. Typical curves of renewable energy data and load data over a typical week. (a) Wind data. (b) PV data. (c) Load data.

B. CV Results of Proposed Method

According to the proposed framework based on the generalized loss function, the CVs of wind and PV units are evaluated from low to high renewable energy penetration levels. To verify the proposed method, several methods are considered.

1) M1: the annual capacity factor of VRE is used as the CV.

2) M2: the capacity factor of VRE during peak load periods is used as the CV.

3) M3: the COPT-based EENS is adopted as the reliability function, and the CV is iteratively solved [2].

4) M4: the proposed generalized loss function and proposed analytical expression in (21) are adopted to calculate the CV.

5) M5: the proposed generalized loss function and the iterative method are adopted to calculate the CV. The result serves as the benchmark.

Figure 5 shows the CV and CC results of a pure wind farm as the installed capacity varies from 100 MW to 3000 MW with steps of 100 MW. It shows that when utilizing the capacity factor-based methods (M1 and M2), the CV result and the installed capacity follow a linear correlation. However, for the other methods, the CV results show saturation as the renewable energy penetration level increases, indicating that the marginal system adequacy provided by the VRE decreases.

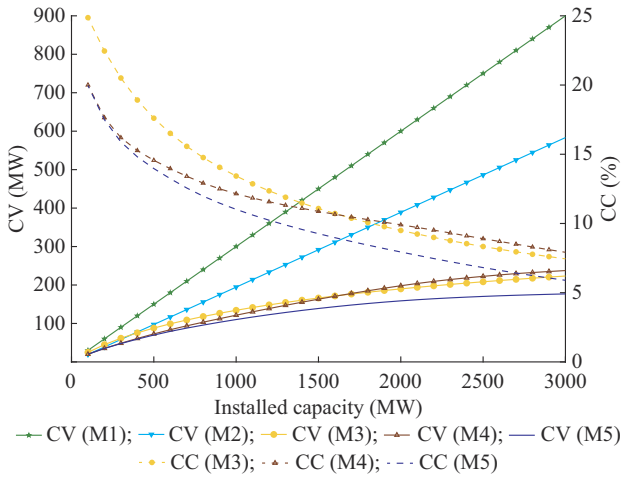

Fig. 5. CV and CC results of a pure wind farm with increasing installed capacity using different methods.

For M4, when the installed capacity is less than 1000 MW, the CV results are quite close to those of M5. In this range, the error of M4 is less than 10%. The corresponding CC result decreases from 20% to 12%. It is also noted that M4 shows a similar CV variation pattern to that of M3. If the installed capacity reaches 2500 MW, the energy generated by the wind farm accounts for 42.8% of the total load. M4 shows that the CV result is 170 MW, and the CC result is 6.8%.

The wind power fluctuation is the main reason for the saturation of the CV. On the one hand, a single near-zero wind power output during the peak load periods Ω will cause significant loss under the generalized loss function with increasing capacity. The critical periods when the loss of load remains high gradually become bottlenecks, and the increased VRE capacity cannot further improve the adequacy. On the other hand, according to the definition of EFC, the VRE generation is supposed to replace part of the existing system adequacy level at the value of P_{cv}. Then, the new net load $d_t^{\text{net}}+P_{\text{cv}}$ would exceed the wind power output w_t during some non-peak load periods in Ω', especially at a high renewable energy penetration level. Under the proposed framework, the two aspects jointly drive the diminishing marginal value of CVs as the renewable energy penetration level in-

creases.

In addition, the CV and CC results with increasing installed capacity of mixed wind and PV resources are also evaluated, as presented in Fig. 6. The capacity ratio of wind resources to PV resources is 1:1. The general variation in the CV of the mixed wind and PV resources with increasing VRE penetration level is consistent with that of a pure wind farm. When the installed capacity is 2500 MW, the renewable energy penetration level is 34.9%. The CV result from M5 is 178 MW, and the CC result is 7.1%. Compared with that of a pure wind farm, the complementarity of wind and PV resources reduces the deviation of VRE generation, which results in an increase in CV. Additionally, the VRE generation of mixed wind and PV resources shows a more positive source-load correlation. For the test data, the Pearson correlation coefficient between PV and load data is 0.39, while for wind and load data, it is –0.04.

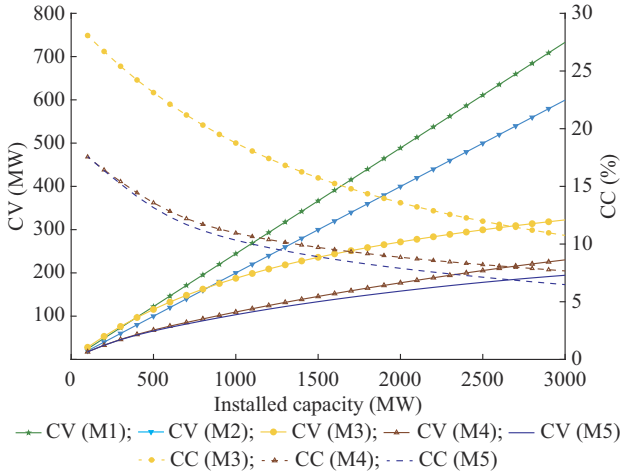

Fig. 6. CV and CC results with increasing installed capacity of mixed wind and PV resources using different methods.

C. Impact Factors on CV

Two impact factors are elaborated upon in this subsection. A total of 2000 MW capacity of mixed wind and PV resources is tested based on the IEEE-RTS79 test system.

1) VRE Generation Variance

Multiple renewable energy generation curves of different VRE generation variances are constructed. It is noted that both the capacity factor and the source-load correlation remain identical in each curve. A constant curve of the capacity factor is first utilized as the zero VRE generation variance case. Then, the difference between the basic wind power output curve and the constant curve is uniformly scaled and added to the constant curve. The target per unit deviations $\sigma(W)/E(W)$ of the generation unit W are set from 0 to 1.2 with steps of 0.2. Any scaled value that exceeds the bounds of 0 to 1.0 p.u. will be modified to be within the bounds. Figure 7 displays the hourly load and VRE generation curves for a typical week. The different VRE generation curves have the same capacity factor but have different VRE generation variances. $\sigma(W)/E(W)=0$ corresponds to the constant value curve.

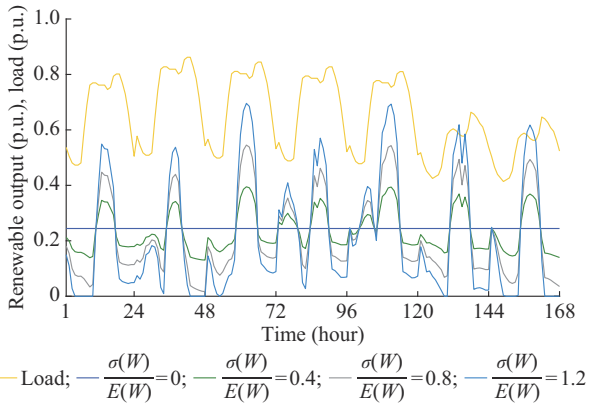

Fig. 7. Hourly load and VRE generation curves with different VRE generation variances for a typical week.

The CVs for VRE are then calculated separately. Some statistical factors derived from the explicit expression (21) are also calculated and listed in Table I. The CVs of VRE are calculated using both M4 and M5. $\rho_{\Omega}(D^N, W)$ denotes the Pearson correlation coefficient between the load and VRE generation during the peak load periods. The capacity factors during the peak periods $E_{\Omega}(W)$ are different due to the scaling process. When the VRE generation variance is zero, the CV of VRE is exactly its annual capacity factor $E(W)$. More importantly, as the VRE generation variance increases, the CV of VRE sharply decreases. It is worth noting that the CV decreases faster than $E_{\Omega}(W)$, indicating the negative impact of the VRE generation variance on its CV. Moreover, when comparing M4 and M5, the results of M4 are closer to the benchmark for low VRE generation variance cases. With increasing VRE generation variance, the relative error is less than 7.2%.

TABLE I
CVs and Some Statistical Factors for Different VRE Generation Variances

$E_{\Omega}(W)$ (MW)	$\frac{\sigma_{\Omega}(W)}{E_{\Omega}(W)}$	$\sigma^2_{\Omega}(W)$	$\rho_{\Omega}(D,W)$	CV of M4 (MW)	CV of M5 (MW)
488.70	0	0	0	488.70	488.70
458.94	0.15	4970	–0.2786	418.56	418.50
429.18	0.33	19900	–0.2786	339.33	337.75
399.42	0.53	44700	–0.2786	254.43	248.48
369.66	0.76	795000	–0.2786	163.91	152.95
342.29	1.02	123000	–0.2823	81.30	77.72
331.32	1.22	163000	–0.2874	44.83	44.18

Figure 8 illustrates the peak load duration curve and the time-corresponding VRE generation for different VRE generation variances. The yellow line shows the net load $d_t^{\text{net}}+P_{\text{cv}}$ during the periods when it is positive. As described in (6), the value of VRE generation that exceeds the net load is corrected by u_t, which is represented by the green line. The load shedding values are also plotted. In low VRE generation variance cases, the VRE generation is relatively stable, as shown in Fig. 7. Thus, the net load is fully supplied by

VRE generation except for some top load periods, and the load-carrying capability increases. However, in high VRE generation variance cases, low-level-generation or even zero-generation periods frequently occur. During these periods, the mismatch between generation and load greatly contributes to the total loss. Under the proposed framework, the CV sharply decreases due to these bottleneck periods.

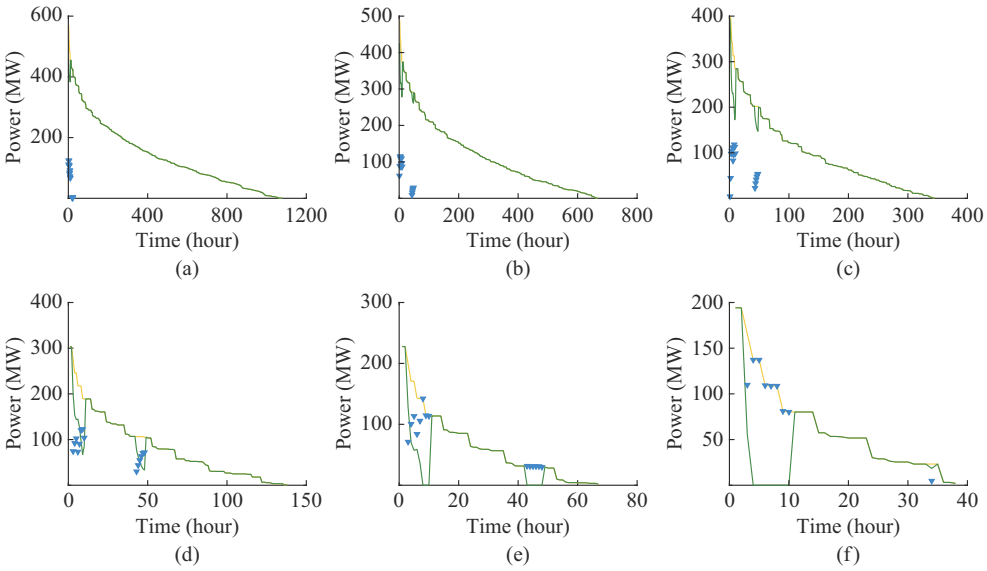

Fig. 8. Peak load duration curve and time-corresponding VRE generation for different VRE generation variances. (a) $\sigma(W)/E(W) = 0.2$ and CV is 418.5 MW. (b) $\sigma(W)/E(W) = 0.4$ and CV is 337.8 MW. (c) $\sigma(W)/E(W) = 0.6$ and CV is 248.5 MW. (d) $\sigma(W)/E(W) = 0.8$ and CV is 152.9 MW. (e) $\sigma(W)/E(W) = 1.0$ and CV is 77.72 MW. (f) $\sigma(W)/E(W) = 1.2$ and CV is 44.18 MW.

2) Source-load Correlation

Multiple source-load correlation cases on the test system are constructed. The chronological ranks of the VRE generation curves are intentionally shifted in different ways so that the capacity factor of VRE and VRE generation variance remain unchanged. In particular, the 365 daily VRE generation curves are reordered in the same rank as the daily average load demand to construct a significant positive correlation case. Similarly, we rearrange the daily VRE generation curves in the opposite rank to load and obtain a case with a significant negative correlation. The basic test curve is denoted as Case A. The positive and negative correlation cases are denoted as Cases B and C, respectively. Figure 9 displays the monthly load and average VRE generation curves in each case.

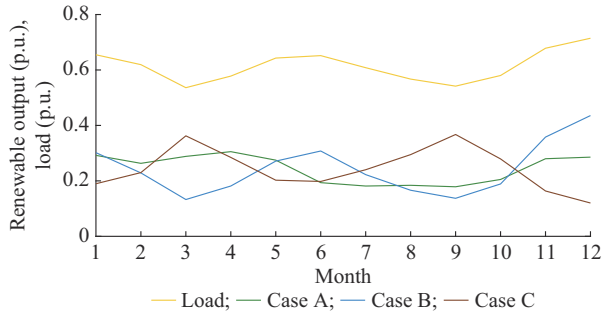

Fig. 9. Monthly load and VRE generation curves for different source-load correlation cases.

For the test system, the CVs and some statistical factors in Cases A-C are calculated and listed in Table II. The two evaluation methods M4 and M5 yield comparable results with relative errors of no more than 12%. A higher correlation coefficient between the VRE generation and load results in a greater CV. In Case B, the abundant VRE generation during peak load periods can properly respond to the capacity requirement, which results in a high CV. It is also worth noting that in Case B, the CV of VRE even exceeds the result from the constant curve, which is 488.70 MW, as displayed in Table I. This demonstrates that the positive correlation with the load of a VRE unit could increase its adequacy contribution beyond its capacity factor. In contrast, due to the weak performance of the VRE during peak load periods in Case C, the calculated CC decreases to nearly 1.1%.

TABLE II
CVs AND SOME STATISTICAL FACTORS IN CASES A-C

Case	$\rho(D, W)$	$E_{\Omega}(W)$ (MW)	$\frac{\sigma_{\Omega}(W)}{E_{\Omega}(W)}$	CV of M4 (MW)	CV of M5 (MW)
Case A	0.22	399.70	0.62	177.09	157.91
Case B	0.61	1315.20	0.22	656.93	587.44
Case C	–0.18	82.37	1.37	22.43	21.33

D. Discussion of Analytical Error

Compared with M5, the approximation of M4 introduces analytical error in power systems with high renewable energy penetration. The overall error is composed of two parts, as proposed in (22). Figure 10 illustrates the two parts in two test cases. With a capacity of 3000 MW, the relative er-

ror is less than 20% for the case with mixed wind and PV resources in Fig. 10(a). Compared with the error from the fraction approximation, the error from the nonpeak loss Δ is the main cause. As the VRE penetration level increases, Δ will also increase. Under the proposed framework, it is ensured that Δ will not exceed the left term $\sum_{t\in\Omega} g_t(0)$ of (9). As displayed in Fig. 10(b), error saturation for the case with a pure wind farm occurs at 3000 MW, which represents a VRE penetration level of more than 50%.

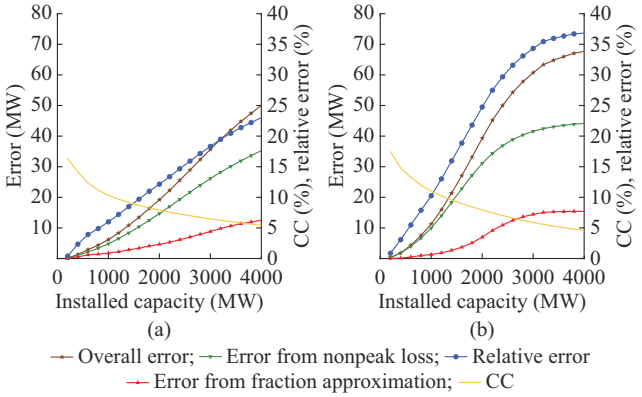

Fig. 10. Decomposition of analytical error in two test cases. (a) Case with mixed wind and PV resources. (b) Case with a pure wind farm.

E. Impact of System Adequacy Level

The CV results are greatly influenced by the current system adequacy level, which is reflected by the value of G in the proposed framework. As presented in Assumption 1, a specific EENS level corresponds to a unique system adequacy level G. Figure 11 shows the CCs of VRE with increasing installed capacity of mixed wind and PV resources at different EENS levels.

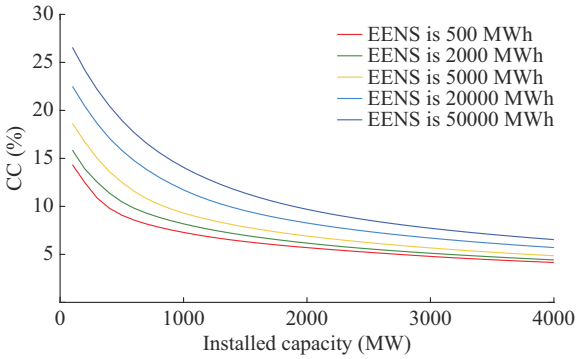

Fig. 11. CCs of VRE with increasing installed capacity of mixed wind and PV resources at different EENS levels.

The capacity ratio of wind resources to PV resources is 1:1. In general, a sufficient system adequacy level indicates less power scarcity, so less capacity margin is available for the mixed wind and PV farm. Therefore, the contribution of VRE to system adequacy is limited in a system with high adequacy compared with a system with low adequacy. As the EENS level increases from 500 MWh to 50000 MWh, the CC of a 100 MW mixed wind and PV farm decreases from 26.6% to 14.3%, which is nearly halved. At a high renewable energy penetration level, the CC of a 4000 MW mixed wind and PV farm drops from 6.5% to 4.2%.

V. Conclusion

Estimating the contribution of VRE to system adequacy is a key concern in power system planning. This paper revisits the conventional CV evaluation methodologies and builds a general CV evaluation framework for power systems with high renewable energy penetration. A generalized loss function is proposed. Through rigorous derivation, an analytical expression of CV under the proposed framework is proposed. The CV of VRE is generally a correction term added to its capacity factor during peak load periods. The installed capacity, VRE generation variance, and source-load correlation dominate this value.

The results of a case study show that the proposed analytical method is as accurate as the iterative method at a renewable energy penetration level of more than 40% of the annual demand. The results illustrate the saturation effect of the CV of VRE with increasing installed capacity. In terms of the impact factors, a larger VRE generation variance and a more negative source-load correlation will both lead to a lower CV. In the IEEE-RTS79 test system, a 2500 MW wind farm (with renewable energy penetration level of 40%) has a CV of 170 MW, and the corresponding CC is 6.8%, which decreases from 20.0% at an installed capacity of 100 MW. For the case with mixed wind and PV resources, the CV at an installed capacity of 2500 MW is 178 MW, and its CC decreases from 17.6% to 7.1% at an installed capacity of 100 MW.

References

[1] B. Frew, W. Cole, Y. Sun *et al*., "8760-based method for representing variable generation capacity value in capacity expansion models," Denver, NREL, Tech. Rep. NREL/CP-6A20-68869, 2017.

[2] A. Keane, M. Milligan, C. J. Dent *et al*., "Capacity value of wind power," *IEEE Transactions on Power Systems*, vol. 26, no. 2, pp. 564-572, May 2011.

[3] E. Zhou, W. Cole, and B. Frew, "Valuing variable renewable energy for peak demand requirements," *Energy*, vol. 165, pp. 499-511, Dec. 2018.

[4] H. Holttinen, J. Kiviluoma, A. Robitaille *et al*., "Design and operation of power systems with large amounts of wind power: final summary report, IEA Wind Task 25, phase two 2009-2011," Espoo, VTT Technical Research Centre of Finland, Tech. Rep., 2012.

[5] T. Mertens, K. Bruninx, J. Duerinck *et al*., "Capacity credit of storage in long-term planning models and capacity markets," *Electric Power Systems Research*, vol. 194, p. 107070, May 2021.

[6] M. Amelin, "Comparison of capacity credit calculation methods for conventional power plants and wind power," *IEEE Transactions on Power Systems*, vol. 24, no. 2, pp. 685-691, May 2009.

[7] M. Milligan and K. Porter, "The capacity value of wind in the United States: methods and implementation," *The Electricity Journal*, vol. 19, no. 2, pp. 91-99, Mar. 2006.

[8] Y. Si, L. Chen, X. Zhang *et al*., "Capacity allocation of hybrid power system with hot dry rock geothermal energy, thermal storage, and PV based on game approaches," *Journal of Modern Power Systems and Clean Energy*, vol. 11, no. 1, pp. 290-301, Jan. 2023.

[9] N. Zhang, Y. Yu, C. Fang *et al*., "Power system adequacy with variable resources: a capacity credit perspective," *IEEE Transactions on Reliability*, vol. 73, no. 1, pp. 53-58, Mar. 2024.

[10] L. L. Garver, "Effective load carrying capability of generating units," *IEEE Transactions on Power Apparatus and Systems*, vol. PAS-85, no. 8, pp. 910-919, Aug. 1966.

[11] K. Dragoon and V. Dvortsov, "Z-method for power system resource adequacy applications," *IEEE Transactions on Power Systems*, vol. 21, no. 2, pp. 982-988, May 2006.
[12] C. J. Dent, A. Keane, and J. W. Bialek, "Simplified methods for renewable generation capacity credit calculation: a critical review," in *Proceedings of IEEE PES General Meeting*, Minneapolis, USA, Jan. 2010, pp. 1-9.
[13] M. A. Abdullah, K. M. Muttaqi, A. P. Agalgaonkar *et al*., "A noniterative method to estimate load carrying capability of generating units in a renewable energy rich power grid," *IEEE Transactions on Sustainable Energy*, vol. 5, no. 3, pp. 854-865, Jul. 2014.
[14] N. Zhang, C. Kang, D. S. Kirschen *et al*., "Rigorous model for evaluating wind power capacity credit," *IET Renewable Power Generation*, vol. 7, no. 5, pp. 504-513, Sept. 2013.
[15] R. Sioshansi, S. H. Madaeni, and P. Denholm, "A dynamic programming approach to estimate the capacity value of energy storage," *IEEE Transactions on Power Systems*, vol. 29, no. 1, pp. 395-403, Jan. 2014.
[16] S. Zachary and C. J. Dent, "Probability theory of capacity value of additional generation," *Proceedings of the Institution of Mechanical Engineers*, *Part O*: *Journal of Risk and Reliability*, vol. 226, no. 1, pp. 33-43, Feb. 2012.
[17] P. Yong, A. Botterud, N. Zhang *et al*., "Capacity value of uninterruptible power supply storage," *IEEE Transactions on Power Systems*, vol. 38, no. 2, pp. 1763-1766, Mar. 2023.
[18] M. Ding and Z. Xu, "Empirical model for capacity credit evaluation of utility-scale PV plant," *IEEE Transactions on Sustainable Energy*, vol. 8, no. 1, pp. 94-103, Jan. 2017.
[19] A. A. Kadhem, N. I. A. Wahab, I. Aris *et al*., "Computational techniques for assessing the reliability and sustainability of electrical power systems: a review," *Renewable and Sustainable Energy Reviews*, vol. 80, pp. 1175-1186, Dec. 2017.
[20] Y. Wang, N. Zhang, C. Kang *et al*., "Ordinal optimization theory based planning for clustered wind farms considering the capacity credit," *Journal of Electrical Engineering and Technology*, vol. 10, no. 5, pp. 1930-1939, Sept. 2015.
[21] D. Dhungana and R. Karki, "Data constrained adequacy assessment for wind resource planning," *IEEE Transactions on Sustainable Energy*, vol. 6, no. 1, pp. 219-227, Jan. 2015.
[22] S. Wang, N. Zheng, C. D. Bothwell *et al*., "Crediting variable renewable energy and energy storage in capacity markets: effects of unit commitment and storage operation," *IEEE Transactions on Power Systems*, vol. 37, no. 1, pp. 617-628, Jan. 2022.
[23] R. M. G. Castro and L. A. F. M. Ferreira, "A comparison between chronological and probabilistic methods to estimate wind power capacity credit," *IEEE Transactions on Power Systems*, vol. 16, no. 4, pp. 904-909, Nov. 2001
[24] Probability Methods Subcommittee, "IEEE reliability test system: a report prepared by the reliability test system task force of the application of probability methods subcommittee," *IEEE Transactions on Power Apparatus and Systems*, vol. PAS-98, no. 6, pp. 2047-2054, Aug. 1979.
[25] Y. Zhou, P. Mancarella, and J. Mutale, "Framework for capacity credit assessment of electrical energy storage and demand response," *IET Generation*, *Transmission & Distribution*, vol. 10, no. 9, pp. 2267-2276, Jun. 2016.
[26] D. Stenclik, A. Bloom, W. Cole *et al*., "Quantifying risk in an uncertain future: the evolution of resource adequacy," *IEEE Power and Energy Magazine*, vol. 19, no. 6, pp. 29-36, Nov. 2021.

Yanghao Yu received the B. S. degree from Tsinghua University, Beijing, China, in 2020. He is currently pursuing the Ph.D degree in electrical engineering from Tsinghua University. His research interests include power system planning and operation, resource adequacy, and capacity value of renewable energy.

Haiyang Jiang received the B.S. degree from Huazhong University of Science and Technology, Wuhan, China, in 2018, and the Ph.D. degree from Tsinghua University, Beijing, China, in 2023. He was a Visiting Student with Harvard University, Cambridge, USA, from February 2022 to August 2022. He is currently a Postdoctoral Fellow at Department of Electrical Engineering, Tsinghua University. His research interests include power system planning, climate risk, and long-duration storage.

Ning Zhang received the B.S. and Ph.D. degrees from Tsinghua University, Beijing, China, in 2007 and 2012, respectively. He is currently a Tenured Associate Professor at the same university. His research interests include renewable energy, low-carbon power system planning and operation, and multi-energy system integration.

Pei Yong received the B. S. and Ph. D. degrees from Tsinghua University, Beijing, China, in 2018 and 2023, respectively. He is currently an Associate Professor at the College of Electrical Engineering, Chongqing University, Chongqing, China. His research interests include power system optimization, energy storage, and distributed resource integration.

Fei Teng received the B.Eng. degree in electrical engineering from Beihang University, Beijing, China, in 2009, and the M. Sc. and Ph. D. degrees in electrical engineering from Imperial College London, London, U. K., in 2010 and 2015, respectively. He is currently a Senior Lecturer with the Department of Electrical and Electronic Engineering. His research focuses on power system operation with high penetration of inverter-based resources (IBRs) and cyber-resilient and privacy-preserving cyber-physical power grid.

Jiawei Zhang received the B.S. degree in mathematics and physics with a minor in computer science from Tsinghua University, Beijing, China, in 2019. He received the Ph. D. degree in electrical engineering from Tsinghua University, in 2024. He is currently working in China Electric Power Planning & Engineering Institute, Beijing, China. His research interests include power system operation, planning, and frequency stability.

Yating Wang received the B.S. and M.S. degrees from Tsinghua University, Beijing, China, in 2008 and 2012, respectively. She is currently working in China Electric Power Planning & Engineering Institute, Beijing, China. Her research interests include power system planning and new energy planning.

Goran Strbac is currently a Professor of energy systems at Imperial College London, London, U. K.. He led the development of novel advanced analysis approaches and methodologies that have been extensively used to inform industry, governments, and regulatory bodies about the role and value of emerging new technologies and systems in supporting cost effective evolution to smart low carbon future. He is currently the Director of the Joint Imperial-Tsinghua Research Centre on Intelligent Power and Energy Systems, leading author in IPCC WG 3, member of the European Technology and Innovation Platform for Smart Networks for the Energy Transition, and a Member of the Joint EU Programme in Energy Systems Integration of the European Energy Research Alliance. His research interests include optimization of operation and investment of low-carbon energy systems, energy infrastructure reliability, and future energy market.